

Radioactivity

Giedrė Astrauskaitė & Sofie Nordahl Erner

03/02/2017

1 Abstract

This report set out to investigate the fundamental properties of radioactivity using a mixed nuclide source and a CASSY 2 unit. The statistical nature of independent radioactive decays was studied through the distributions of background radiation and radiation from source with or without shielding. Alpha, beta and gamma radiation types were compared in terms of their penetrating ability and it could be shown that alpha was stopped by 20 μm aluminium, beta by 5-6 mm aluminium, and gamma heavily reduced by 1 cm of lead. A theoretical estimating of the dose received during time in laboratory was done. Likewise, safety of the experiment and the accuracy of the results was assessed.

2 Introduction

Living organisms are constantly exposed to ionizing background radiation due to radioactive isotopes existing in their food and surroundings. In science, man-made ionizing radiation is of great importance as it is used in medicine for CT or X-ray scans, producing electricity in nuclear power plants, and sterilizing food or medical equipment. However, such use of radioactive materials raises acute safety issues: currently there is no effective solution to the nuclear waste storage problem and even with very small chance of occurring, nuclear accidents pose a significant hazard. Hence, it is important to work towards solutions of the aforementioned issues. In the following experiment the fundamentals of radioactivity were studied. Radiation count rate was measured using a Geiger-Müller counter in order to understand the statistical nature of radioactive decay, compare the background radiation to that of an unshielded source and investigate how alpha, beta and gamma radiation are absorbed when they interact with matter. In addition, theoretical estimation of radiation dose received during the laboratory session was carried out and doses from various sources were compared while discussing the safety of such exposure.

3 Background Theory

Fewer than 300 of 2500 known nuclides are stable [1]. The nuclei of the unstable atoms have excess energy and so in order to achieve the most energetically favourable state particles or electromagnetic radiation are emitted. Consequently, other nuclides are formed. This process is defined as radioactive decay and the nuclei that emit energy are classified as radioactive. Radioactive decay is spontaneous as it occurs without any interaction with other atomic constituents. As the prediction of when a given nucleus will decay is unattainable, radioactive decay is a stochastic process at the level of single atoms. This process is governed by equation (1) where N is the number of nuclei left after some time t has elapsed, N_0 the initial number of nuclei and λ the decay constant.

$$N = N_0 e^{-\lambda t} \quad (1)$$

The decay constant can be used to find the half-life which describes the time it takes for half of the nuclei in any sample to decay. Some radioactive materials have very long half-lives compared to others; for instance, Polonium-215 has a half life of 0.0018 seconds while Uranium-238 radioisotope has a half life of 4.5 billion years [2].

Radiation can be classified as non-ionizing and ionizing. Non-ionizing radiation has longer wavelengths and therefore less energy. On the contrary, ionizing radiation carries enough energy to damage cells by knocking the electrons out of their orbit. Therefore it poses mutagenic hazard to living organisms as the cells can die or become cancerous. There are three types of ionizing radiation that are most common, namely alpha, beta, gamma decays [1]. Radiation can be artificial (for instance, the source used in this laboratory, radiation due medical imaging like CT-scan, etc.) or natural. The types account for 18.6% and 81.4% of total average annual exposure respectively. Natural sources of background radiation include cosmic rays, radiation from the core of the earth, various substances in food or human body. In particular, inhaling radon gas causes 36.6% of annual exposure. Overall, the exposure due to the aforementioned natural and artificial sources accounts for approximately 2.4 mSv per year per person [3].

Alpha Decay

An alpha particle is a He-4 nucleus, containing two protons, two neutrons and has spin 0. This decay mainly occurs when the nuclei are too heavy to be stable. The trajectory of an alpha particles bends in magnetic and electric fields such that a positive charge is indicated. [1]

Beta Decay

Beta decay is classified as beta plus, beta minus and electron capture as described in Table 1:

β^-	β^+	Electron Capture
$n \rightarrow p + e^- + \bar{\nu}_e$	$p \rightarrow n + e^+ + \nu_e$	$e^- + p \rightarrow n + \nu_e$

Table 1: Beta Decay Classification. Source: [1]

Under the influence of magnetic and electric fields the trajectory of the beta particle (electron in case of beta minus and positron in case of beta plus) will be bend indicating the positive charge of a positron and negative charge of an electron [1].

Gamma Decay

Gamma decay occurs when a nucleus is in an excited state and bombardment with high-energy particles causes it to decay to the ground state via emission of one or more photons (gamma rays). Hence, Gamma rays are emitted from the nuclei when the nucleons change their energy state. Gamma does not bend in electric or magnetic fields and hence is electrically neutral [1].

The aforementioned types of radiation have different abilities to penetrate materials as displayed in Figure 3. While alpha particles are stopped by a sheet of paper and beta by aluminium foil, the majority of gamma rays can be blocked by a lead barrier. This property of α , β and γ will be further investigated in the experiment.

Absorption of Radiation

The absorption of radiation is given by equation (2) where A is the activity detected, x is the thickness of the absorber, μ is the absorption coefficient of the used material and A_0 is the activity at $x = 0$ [3].

$$A = A_0 e^{-\mu x} \quad (2)$$

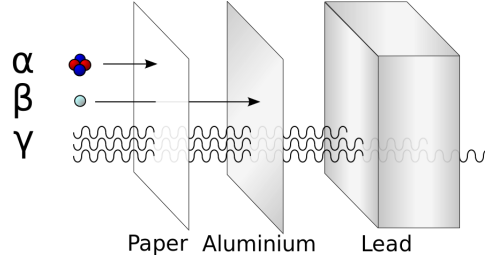


Figure 1: Schematic diagram of ability of α , β , and γ radiation to penetrate matter. Source: [4]

Means to Measure Radiation

In the experiment, a Geiger Müller counter was used to measure ionizing radiation (Figure 2). The device has a cylindrical container filled with low pressure argon gas. Likewise, a wire of positive potential, is placed along the axis of a tube, which is at negative potential. High voltage is adjusted resulting in a strong electric field between the aforementioned constituents. Once α , β or γ -ray passes through the tube it causes ionization and hence electrons and ions are produced. Consequently, for a brief moment, a discharge of current is triggered and flows in the circuit. Then it is amplified and counted by a scaler or ratameter. After a certain time, known as the dead time of the counter, the ions disperse and the counter becomes active again. [3]

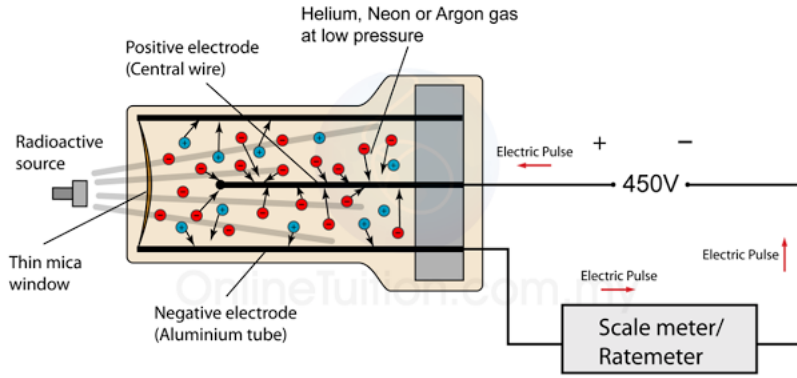


Figure 2: Geiger - Müller Apparatus. Source: [5]

Statistical Nature of Radioactive Decay

Radioactive decays happen spontaneously and will occur at a fixed probability per unit time. This process can be described using the Poisson distribution which expresses the probability of a number of discrete event occurring in a fixed time. This relationship is given by equation (3).

$$P(A) = e^{-\bar{A}} \cdot \frac{\bar{A}^A}{A!} \quad (3)$$

where \bar{A} is the average number of events and A is the total number of event counted. The average number of events is calculated using formula (4) and the sample standard deviation by formula (5).

$$\bar{A} = \frac{1}{A_{total}} \cdot \sum_i A_i \quad (4)$$

$$\sigma_{A_{total}} = \sqrt{\frac{1}{A_{total} - 1} \cdot \sum_{i=1}^{A_{total}} (A_i - \bar{A})^2} \quad (5)$$

As the decay of isotopes are independent, one can separate and use the following property of the Poisson distribution where λ_1 and λ_2 are independent variables measured n times as in equation (6).

$$P(n, \lambda_1 + \lambda_2) = P(n, \lambda_1) + P(n, \lambda_2) \quad (6)$$

The mean count rates (λ) of α, β, γ and background can be determined using equation (7). The aforementioned distribution is the sum of α, β, γ and background event distributions. The variances (σ)² add up similarly as in equation (8) [3].

$$\lambda_{\alpha+\beta+\gamma+bg} = \lambda_{\alpha} + \lambda_{\beta} + \lambda_{\gamma} + \lambda_{bg} \quad (7)$$

$$\sigma_{\alpha+\beta+\gamma+bg}^2 = \sigma_{\alpha}^2 + \sigma_{\beta}^2 + \sigma_{\gamma}^2 + \sigma_{bg}^2 \quad (8)$$

4 Experimental Method

The experiment was conducted using a CASSY unit in order to take measurements of the background count rate. For the Geiger Müller readings to be accurate, the source was kept remotely from the detector. The necessary adjustments were made using the data logger/computer in CASSY 2 Lab software and 300 readings were taken with intervals of 1 second. As it is essential for the detector to reset after each measurement, a delay occurs. To make up for the dark-time the measuring time was set to 361 seconds. The results then were exported to a .txt file and MATLAB was used for further analysis.

The same method was used to investigate the activity of α, β and γ radiation. The source of mixed nuclides, containing Am-241, Sr-90 and Cs-137 with activities 4.4 kBq, 4.4 kBq and 7.4 kBq respectively (decay schemes are displayed Appendix 1) [6], was prepared for measurements by removing it from the protective holder and then placing it the holder cylinder. The source was placed in the mounted clip so that it could be kept very close and just in front of the Geiger Müller counter. The described experimental setup is displayed in Figure 3. Once again, 300 readings were taken, ensuring that the readings are higher than the background count rate. To investigate the penetrating ability of α, β and γ radiation, different materials were inserted in between the source and the Geiger-Muller counter.

To stop alpha particles, firstly a sheet of paper and thereafter a piece of aluminium foil of thickness of 20 micrometers was carefully inserted in the end cap. In both cases, 300 readings were taken. To investigate the absorption of beta particles thicker aluminium foil was used. Starting from four pieces of 0.1mm thickness, 180 readings were taken each time after increasing the barrier by increments of 0.4mm until 8mm were reached.

The absorption of gamma radiation and the absorption coefficient of lead was studied as follows. Lead foil pieces were placed in the end cap by increments of 1 mm until 1 cm thick barrier was formed between the Geiger-Muller tube and the source. For each thickness, 300 readings were taken. Theoretical research and mathematical estimation of doses from various sources of radiation was afterwards conducted.

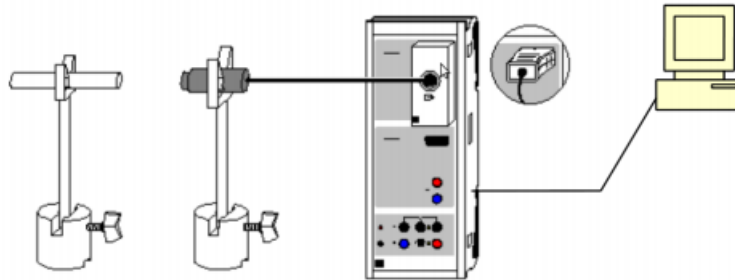


Figure 3: Schematic diagram of the experimental setup. Source: [3]

5 Results & Analysis

The mean and standard deviation of the measurements was found by creating a function in MATLAB which given a column vector with the measurements as entries calculates the mean by summing the entries and thereafter dividing by the total number of entries. The standard deviation was found using equation (5) in a loop. The function can be seen in Appendix 2.

5.1 Background Radiation & Source Without Shielding

The mean and standard deviation of the background radiation, the radiation from the source without shielding and shielded by paper or 20 μm aluminium are displayed in Table 2. Here one can see that the mean for paper and 20 μm aluminium are similar though the mean for the aluminium is higher. While the paper is much thicker than the aluminium, their stopping abilities are alike which is due to the internal structure of each. Even though the paper stopped more alpha particles, the results from the 20 μm aluminium will be used for further calculations due to similarities with the investigation of the penetrating abilities of β which will be performed using aluminium.

	Background Radiation	Radiation source	20 μm Aluminium	Paper
Mean ($\frac{\text{counts}}{\text{second}}$)	0.2233	335.9100	190.3522	179.4867
Standard Deviation ($\sqrt{\frac{\text{counts}}{\text{second}}}$)	0.4832	16.8177	13.0352	11.9804
$\frac{\text{Mean}}{(\text{StandardDeviation})^2}$	0.9564	1.1877	1.1203	1.2505

Table 2: Results from analysis of measurements of background radiation and source.

The histograms for these measurements together with the Poisson distribution for the corresponding mean were plotted using equation (2) and can be seen in Figure 5. As the histograms fit the Poisson graphs, both measurements follow the Poisson Distribution. However, the graph for background radiation is asymmetrical, while the source distribution tends towards a bell curve. As seen in Appendix 3, the Poisson distribution is asymmetrical for small mean values and becomes more and more like the Gaussian as the mean increases; hence the histogram of the source resembles both distributions. This phenomena is explained by the Central Limit Theorem, which states that any sufficiently large sample size will naturally tend to a normal (Gaussian) distribution. The main difference between the Gaussian and the Poisson distributions is that the Gaussian distribution is continuous whereas the Poisson is discrete, hence the Poisson distribution describes our data most accurately [7]. In this experiment, the number of counts can not be negative. The mean of background radiation is 0.233 counts per second and discrete values are measured. Hence the majority of the measurements were at 0 counts per second causing asymmetry in the histogram.

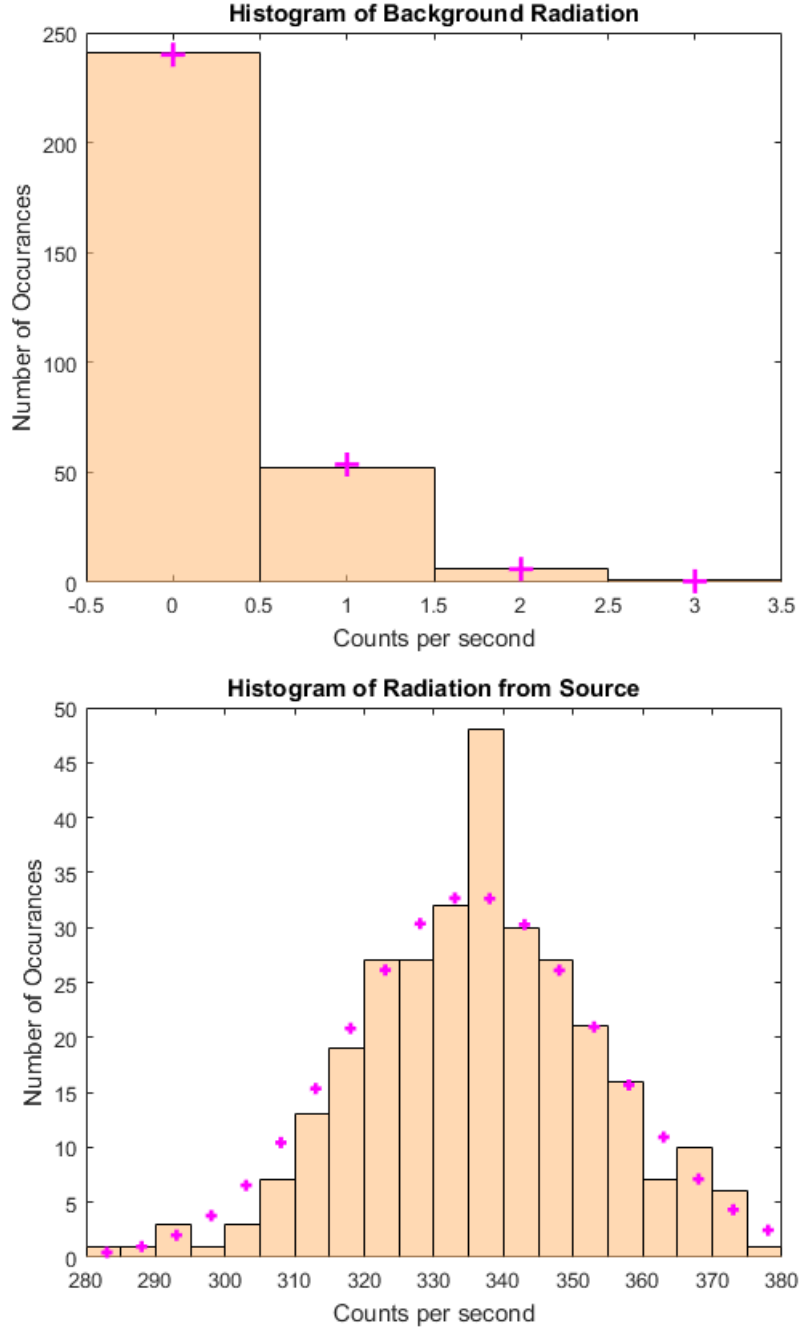


Figure 4: Histograms of Background Radiation & Radiation from Source with the Poisson distribution for the corresponding mean is plotted (refer to purple data-points).

The results from the source shielded by 20 μm aluminium are displayed in Table 2, the histogram of the measurements in Figure 5 and these will later be used to calculate the mean contribution of each type of radiation to the total count rate of the source.

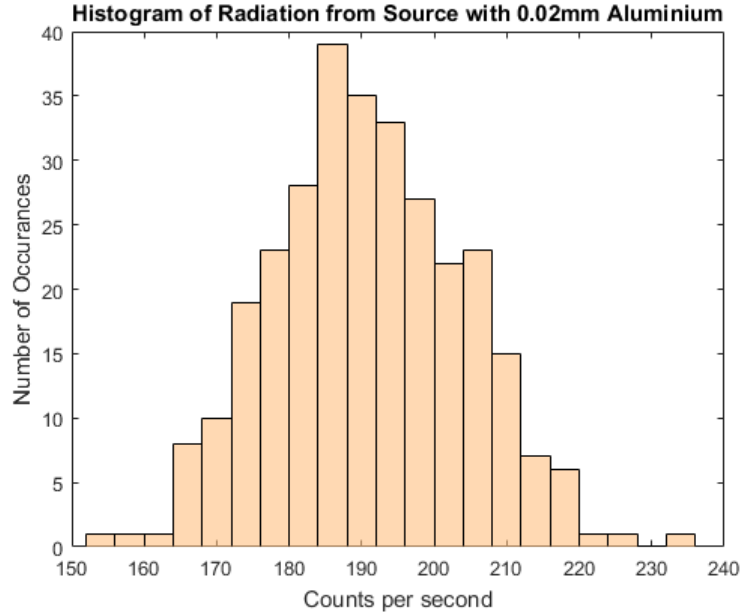


Figure 5: Mean of radiation as a function of thickness of Aluminium.

5.2 Beta Absorption

The measurements obtained with varying thickness of aluminium are displayed in Appendix 4. In Figure 6, the mean of radiation as a function of the thickness of aluminium is shown. The graph depicts how there is a distinct drop in counts per second and thereafter a decreasing decline towards 10 counts per second. It is visible that a significant majority of particles are stopped when going from 0 mm to 0.4 mm which matches the predicted absorption of α particles, and in the interval $[0.4, 6]$ particle count is further reduced. This suggest the stopping of β particles where only γ radiation would remain.

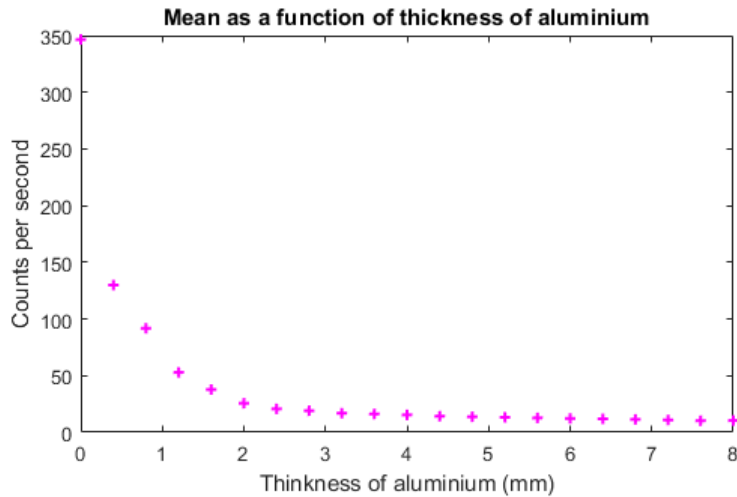


Figure 6: Mean of radiation as a function of thickness of Aluminium.

The shielding thickness of aluminium is 5.21 mm [8]. The histogram for this can be seen in Figure 7 and the corresponding mean and standard deviation can be seen in Appendix 4. These values will be used for further calculation of the count rates for the different types of radiation.

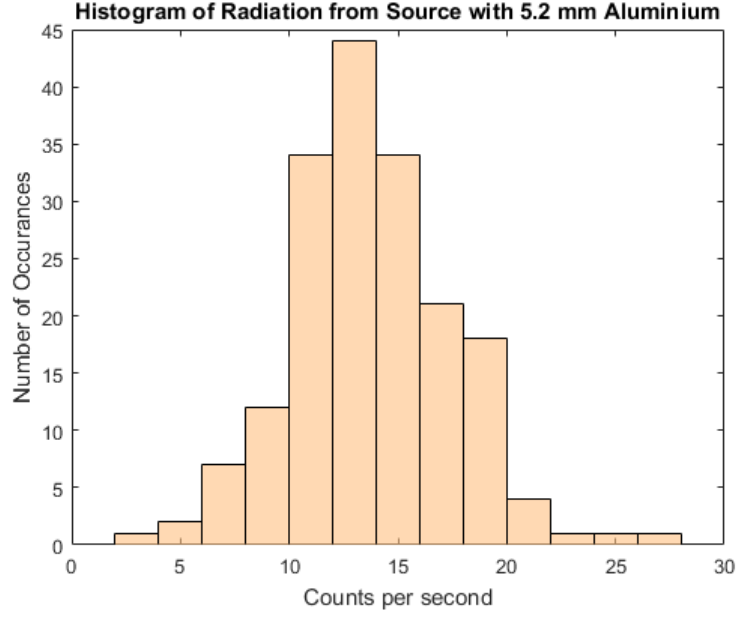


Figure 7: Histogram of Radiation from the Source Shielded by 5.2 mm Aluminium.

5.3 Mean, Standard Deviation & Variance

The mean and standard deviation of the background and total radiation from the source were calculated from the measurements. This together with the results from the measurements obtained through varying thickness of aluminium and lead as seen in Appendix 4 and Appendix 5 can be used to calculate the mean and standard deviation of alpha, beta and gamma radiation from the source using equation (7).

$$\lambda_{\alpha} + \lambda_{\beta} + \lambda_{\gamma} + \lambda_{bg} = 335.91 \quad \lambda_{\beta} + \lambda_{\gamma} + \lambda_{bg} = 179.4867 \quad \lambda_{\gamma} + \lambda_{bg} = 13.3278 \quad \lambda_{bg} = 0.2233$$

These equations give the results for mean values for the different radiation types seen in Table 3. Using the standard deviation acquired in the experiments, the standard deviations for each radiation type can be calculated using equation (8). All standard deviations are relatively small compared to the corresponding means hence the readings are gathered in a small range which suggests accuracy. The mean/variance values (Table 3), found using the values of standard deviations, are all around 1 hence $\lambda_x \approx (\sigma_x)^2$ and the measurements have little deviance from the expected values.

Radiation Type	Mean $\frac{\text{counts}}{\text{second}}$	Standard Deviation $\sqrt{\frac{\text{counts}}{\text{second}}}$	$\frac{\text{Mean}}{(\text{StandardDeviation})^2}$
Source	335.9100	16.8177	1.1877
α	145.5578	3.7825	1.12891
β	177.0244	156.6961	1.1297
γ	13.1045	3.1528	1.0091
Background	0.2233	0.4832	0.2335

Table 3: Mean, Standard Deviation & Mean/Variance for the different types of radiation.

5.4 γ Absorption

The measurements from the experiment with varying thickness of lead can be found in Appendix 5. Equation (2) was re-expressed and used to plot the graph in Figure 9 where the thickness of the lead is on the x-axis whilst the natural logarithm of the corresponding activity is on the y-axis. Formula 9 is the regression for the relationship between $\ln(A)$ and thickness of lead which gives an activity of $e^{3.2045} = 24.6432$ which describes the activity at 0mm of lead which should be equal to the mean of gamma radiation. Our calculated value of the mean of gamma radiation in the previous section was 13.1045 which is smaller than the value calculated here. But as seen on Figure 9, the standard error on the measurements is substantial and results in a range of initial activity of [3,3.5] which results in a mean gamma radiation in the interval [20,33] counts per second. The error bars were calculated using the formula $Q = \ln(x) \rightarrow \sigma_{m,f} = \frac{\sigma_{m,x}}{x}$ [7] and the calculated standard deviation for the measurements. The absorption coefficient of lead can be found using equation (2), hence the value is $0.18867 \frac{1}{mm}$. Figure 8 depicts how the activity decreases to a value of 3.8833 counts per second at 1 cm of lead which is in line with the theory of gamma being stopped by several centimeters of lead [9].

$$\ln(A) = -0.18867 * x + 3.2045 \quad (9)$$

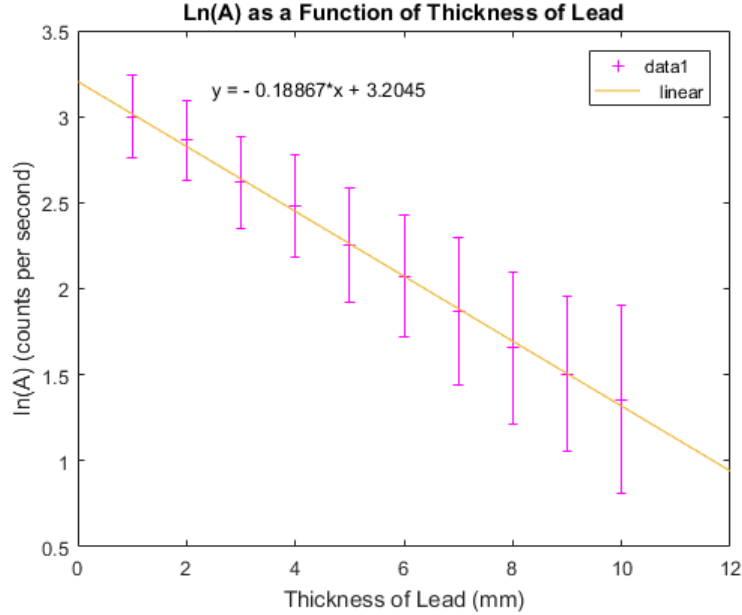


Figure 8: $\ln(A)$ as a function of the Thickness of Lead.

6 Discussion

Theoretical Dose Estimation

As stated before, food is a significant source of radiation. In particular, the common banana is rich in potassium which usually contains 0.0117% of the radioactive ^{40}K [3]. In this theoretical part of the experiment it was verified that a dose received by eating one 150 g banana is $0.1 \mu\text{Sv}$ as follows. Firstly, the potassium content in one 150 g banana is 537 mg. For simplicity the calculations and results are explained in Table 3. As it is determined that $9.674 \cdot 10^{17}$ nuclei of radioactive potassium are present in 150 g banana, the equivalent dose of eating the banana is $0.08(5) \mu\text{Sv}$ or approximately $0.1 \mu\text{Sv}$. As cosmic radiation accounts for 14.4% of total annual dose and hence is 0.35 Sv , it would be necessary to eat 3500 bananas to account for the similar exposure [10].

Constants	Equation	Result
$M_{\text{Kmol}} = 39.0983 \frac{\text{g}}{\text{mol}}$	$n = \frac{m}{M_{\text{Kmol}}}$	$n = 1.60694 \cdot 10^{-6} \text{ moles}$
$N_A = 6.02 \cdot 10^{23} \frac{\text{nuclei}}{\text{mole}}$	$N = N_A \cdot n$	$N = 9.673814702 \cdot 10^{17} \text{ nuclei}$
$t_{\frac{1}{2}} = 1.251(3) \cdot 10^9 \text{ years}$	$N = N_0 e^{-\lambda t}$	$\lambda = 1.75799 \cdot 10^{-17} \text{ s}^{-1}$
-	$A = \lambda \cdot N$	$A = 17.0434476 \text{ Bq}$
$\text{CEDE} = 5.025 \cdot 10^{-9} \frac{\text{Sv}}{\text{Bq}}$	$\text{Dose} = \text{CEDE} \cdot A$	$\text{Dose} = 0.08555 \mu\text{Sv}$

Table 4: Results and calculations for the estimation of the absorbed dose after eating one banana.

To estimate the dose absorbed during this laboratory experiment, several key aspects need to be considered. Firstly, alpha, beta and gamma radiation have different ranges in air. Alpha and beta particles travel up to approximately 3-5 and 15 centimeters in air respectively and hence, exposure to alpha and beta radiation could only have occurred when handling the source by hands. It is assumed that gammas affect half of our body [11]. It is assumed that we have spent 7 hours in the lab and both handled the source for the same amount of time which was approximately 7 minutes. The effective dose can be calculated using the formula: Effective Dose = Absorbed Dose x Relative Biological Effectiveness. Referring to the mean count rates of different types of radiation discussed in section 5.3 and the decay energies of the mixed nuclide source used, displayed in Appendix 1, and taking into account the RBE of alpha, beta and gamma (20, 1 and 1 respectively [12]) the following doses are acquired. The effective dose of alpha was $0.88 \mu\text{Sv}$, 16 pSv for beta, 53 pSv for gamma and the resulting maximum possible effective dose of $0.89 \mu\text{Sv}$ or approximately $1 \mu\text{Sv}$, making alpha the most significant contributor. In reality, this dose is most likely to be smaller as the source was handled with care. The aforementioned dose of $1 \mu\text{Sv}$ is negligible and is the same as the dose received by eating 10 bananas. Hence, it constitutes 0.042% of the average dose absorbed by humans in one year (2.4mSv) and 0.29% of the yearly dose received from cosmic rays. Overall, the dose received during the laboratory session does not pose any hazard to human health.

Note that alpha particles have higher ionising ability and they are stopped easily by a sheet of paper. Hence, they lose all their energy in a very short range. Therefore, if ingested, compared with gamma, they are of a considerably bigger danger to human health as radiation impacts one region very strongly rather than distributes lesser damage in a bigger region. However, if the source is relatively far, gammas pose a bigger threat to human health as they are difficult and their range is large. To reduce the exposure during the laboratory, session the distance from the source should be increased and a protective cylinder of greater stopping power could have been used.

Comparison with other groups

Results were acquired from 2 other groups doing the same experiment which are displayed in Table 5. The mean values for the sources were different which resulted in the measurements of the different types of radiation to vary. Because of this an analysis based on the contribution of the alpha, beta, gamma and background radiation to the total radiation from the source was performed and can be seen in Table 6. The background radiation should have been the same for all groups since all experiments were carried out within the same relatively small area. Though as seen in the results, this was not the case. That suggests differences in effectiveness of Geiger Müller tubes or that the two more similar measurements were taken after the first group had gotten their radioactive source. Two groups had very similar results all over whilst the third had a much more active source resulting in a higher mean value for alpha specifically.

Mean ($\frac{\text{counts}}{\text{second}}$)	Group 1	Group 2	Our Results
Source	412.8800	332.8187	335.9100
Alpha	253.1500	146.3867	156.4233
Beta	146.4977	173.1634	166.1589
Gamma	13.2323	13.6412	13.1045
Background	0.2577	0.2577	0.2233

Table 5: Results from other groups. Source: [13] & [14]

The following table depicts the means for the different types of radiation's contribution to the total radiation measured. This is calculated by dividing the mean for each type by the mean of the source and hence the percentage of the source radiation (PSR) was calculated for the results from each group. The calculations were compared by finding the average and standard deviation which shows that all percentages of the total radiation were within 20% of one-another for each type of radiation.

Type of Radiation	PSR (Our Results)	PSR (Group 1)	PSR (Group 2)	Average PSR	Standard Deviation
Alpha	43.3324	61.3132	43.9839	49.5432	8.3269
Beta	52.7000	35.4195	52.0293	46.7163	7.9927
Gamma	3.9012	3.3028	4.0987	3.7676	0.3384
Background	0.0665	0.0613	0.0774	0.0684	0.0067

Table 6: Analysis of Results from Other Groups.

Error Analysis

Throughout the experiment, there were both systematic and statistical errors. The background radiation is not constant and hence there is a statistical error since one reading will have up to 3 more counts per second than another. This does not result in a great difference when measuring the total radiation from the source or when the source was shielded by aluminium since the average readings were much greater than the uncertainty from the background radiation. On the contrary, the means of the radiation from the source shielded by more than 5 mm lead are all under 10 counts per second where 3 counts per second constitutes a significant difference in measurements. This statistical error would have altered the absorption coefficient of lead and may have lead to an average gamma radiation close to the one found through previous calculations. To understand the origin of systematic error, it is important to note that while gamma radiation is highly penetrating, its ionizing ability is low. Therefore, approximately 99% of this radiation passes through the counter undetected. Consequently, the mean number of counts per second 13.1045 determined in section 5.3 of gamma is very low compared to the actual number of gammas appearing in the surroundings due to the source. If only 1% of gamma rays are detected, the number of counts per second was likely to be $1310.45 \frac{\text{counts}}{\text{second}}$. On the contrary, most of alpha and beta particles should be detected; however, the activity of the source was said to be 16.2 kBq by the manufacturers which is much larger than the 335 Bq measured in this experiment. Hence the inaccuracy might have occurred due to the age and quality of the detector or the source. In general, Geiger Müller counter provides very little information about the particles that trigger it, as the signal is of the same size regardless of type of radiation. The accuracy of this experiment can be increased by choosing a scintillation detector which is more sensitive to gamma radiation. Likewise, for similar results and considerably improved energy resolution, solid state detectors can be used [15]. In addition, a more precise result with more descriptive histograms can be obtained by increasing the number of measurements.

7 Conclusion

Histograms for background and source radiation both resembled Poisson distribution and their shape can be explained by Central Limit Theorem. The mean count rates were found to be 145.5, 177.2, 13.1 per second for alpha, beta, gamma respectively and their sum represented the mean count rate of 335.9 of the source. It was verified that most alpha particles can be stopped by 20 μm aluminium, beta by aluminium of thickness 5-6 mm. The majority of gamma rays were stopped by 10 mm of lead with an absorption coefficient found to be 0.1887 as their count rate dropped from 13.1 to 3.9. Compared with other groups, the contribution from the various types of radiation were majorly alpha and beta contributing approximately 50% each. All three sources considered, gamma radiation counts were very low compared to alpha and beta due to Geiger-Muller counter being insensitive to gamma rays. The estimated dose of 1 microSv absorbed during the experiment poses no significant threat and is 6.5 times lesser than the average daily background radiation dose.

References

- [1] Young, Hugh D. & Freedman, Roger A. *Sears and Zemansky's University Physics with Modern Physics Technology Update*. Pearson Education Limited 2014.
- [2] NDT Resource Center *Radioactive Half-Life*
<https://www.nde-ed.org/EducationResources/HighSchool/Radiography/halflife2.htm>
Visited 31/01/2017
- [3] *Radioactivity Lab Script*.
University of Glasgow 2017.
- [4] Wikipedia: *Radiation*.
<https://en.wikipedia.org/wiki/Radiation>
Visited 22/01/2017
- [5] OnlineTuition.com.my: *Geiger - Müller Tube*.
<http://spmphysics.onlinetuition.com.my/2013/08/geiger-muller-tube.html>
Visited 22/01/2017
- [6] LD DIDACITC *Introduction sheet 559 845*
- [7] Hamilton, David *Mathematical Techniques Lecture Notes*.
University of Glasgow 2016.
- [8] Wolfram Alpha "*Stopping power aluminium, 2.28MeV electron*"
<https://www.wolframalpha.com/input/?i=stopping+power+aluminium,+2.28MeV+electron>
Visited 27/01/2017
- [9] BBC GCSE Bitesize: *Nuclear Radiation*
http://www.bbc.co.uk/schools/gcsebitesize/science/ocr_gateway_pre_2011/living_future/4_nuclear_radiation1.shtml
Visited 29/01/2017
- [10] The Scottish Government "*Key Scottish Environment Statistics 2015: Radioactivity*"
<http://www.gov.scot/Publications/2015/09/4066/318457>
Visited 02/02/2017
- [11] Institute of Physics (IOP): "*Nature of Ionising Radiations*"
<http://practicalphysics.org/nature-ionising-radiations.html>
Visited 01/02/2017
- [12] Eklund, Lars *Nuclear and Particle Physics Lecture Notes (Lecture 2, Radiation)*.
University of Glasgow 2017.

- [13] Terry Millen & Davies, Ross *Radioactivity*
University of Glasgow 2017
- [14] Hargreaves, Rebehak & Walczyk, Weronika *Radioactivity*
University of Glasgow 2017
- [15] Encyclopedia.com *Particle Detectors*
<http://www.encyclopedia.com/literature-and-arts/biographies/english-literature-19th-cent-biographies/radiation-detectors>
Visited 27/01/2017
- [16] Wikipedia: *Normal Distribution*
https://en.wikipedia.org/wiki/Normal_distribution
Visited 25/01/2017
- [17] Wikipedia: *Poisson Distribution*
https://en.wikipedia.org/wiki/Poisson_distribution
Visited 25/01/2017

8 Appendix

8.1 Appendix 1

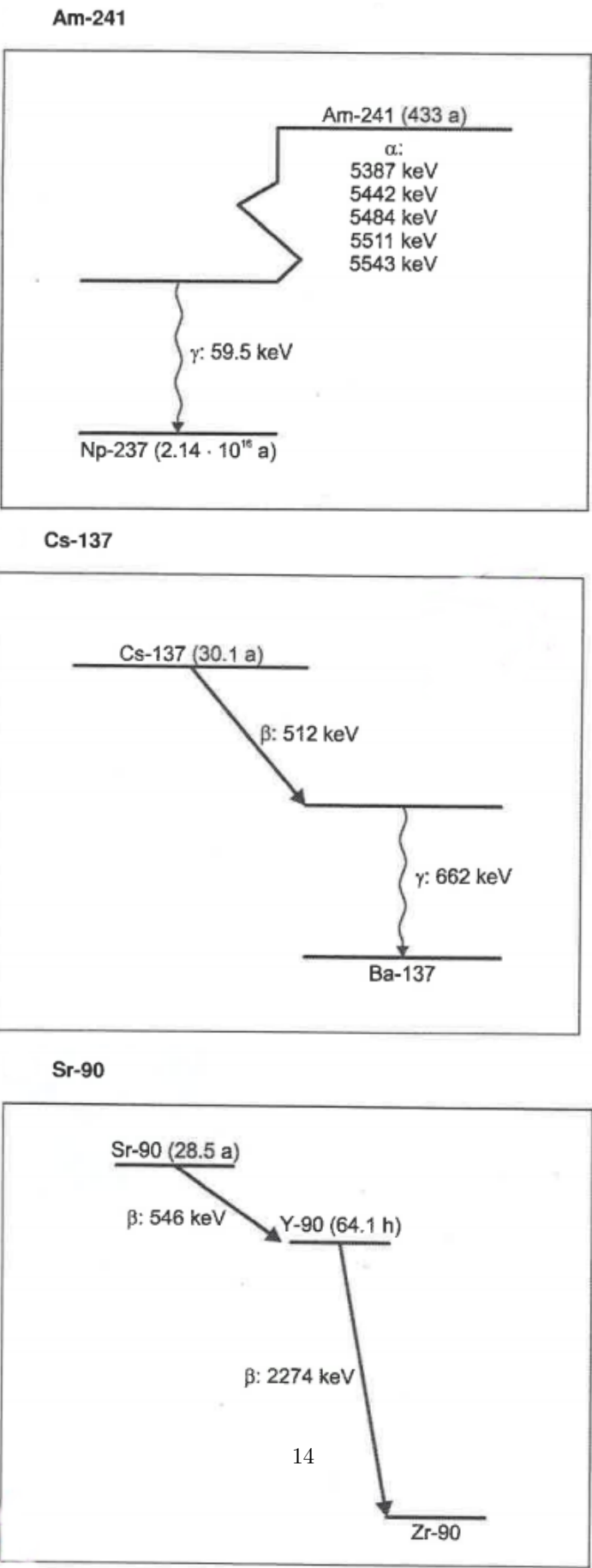


Figure 9: Diagrams of Decays of Isotopes in the Source.
Decay of the most of the source with the radiation of 45 MeV from Am-241 and the β of 546 keV of

8.2 Appendix 2

```
function [mean, sigma_N] = myfunc(A)
% This function will calculate the mean given a coloum of data results

N = size(A,1);
S = sum(A);
mean = (1/N)*S

% Standard Deviation
% sigma_Atotal-1 = sqrt(1/(Atotal - 1) * sum((A_i - mean)^2)

i = 1;
a = A;

while i <= size(A,1)
    a(i) = (a(i) - mean)^2;

    i = i + 1;
end

sigma_N = sqrt((1/N) * sum(a))
end
```

Figure 10: Function in Matlab used to calculate mean and Standard Deviation

8.3 Appendix 3

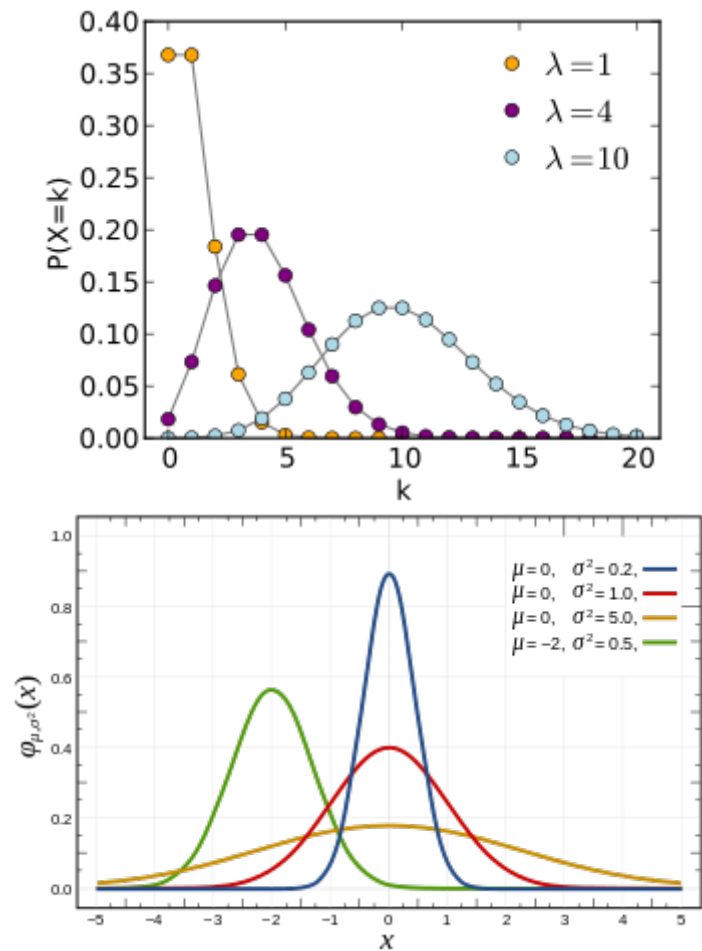


Figure 11: Poisson & Gaussian Distribution. Source: [16] & [17]

8.4 Appendix 4

Thickness of Aluminium (mm)	Mean ($\frac{\text{counts}}{\text{second}}$)	Standard Deviation($\sqrt{\frac{\text{counts}}{\text{second}}}$)	Variance	Mean/Variance
0.0	346.45	18.6203	346.7156	0.9992
0.4	129.8722	11.0991	123.1892	1.0542
0.8	91.8889	9.7627	95.3099	1.5771
1.2	52.9444	7.6331	58.2636	1.5185
1.6	37.8389	5.9078	34.9018	1.6628
2.0	25.7667	4.7704	22.7567	1.0089
2.4	20.7111	5.0536	25.5388	0.9980
2.8	19.0556	4.5555	20.7525	0.9298
3.2	16.9833	4.5270	20.4942	1.0685
3.6	16.1667	3.9868	15.8944	1.0171
4.0	15.4056	3.9408	15.5300	0.9920
4.4	14.2778	3.6149	13.0673	1.0926
4.8	13.6833	3.7245	13.8719	0.9864
5.2	13.3278	3.6360	13.2203	1.0081
5.6	12.7889	3.4010	11.5665	1.1057
6.0	12.1889	3.3213	11.0310	1.1050
6.4	12.0111	3.7535	14.0888	0.8525
6.8	11.4278	3.5340	12.4892	0.9150
7.2	10.9111	3.0300	9.1810	1.1884
7.6	10.3167	3.3224	11.0386	0.9346
8.0	10.4667	3.1595	9.9822	1.0485

Table 7: Results from analysis of measurements of absorption of alpha particles

8.5 Appendix 5

Thickness of Lead (mm)	Mean ($\frac{\text{counts}}{\text{second}}$)	Standard Deviation($\sqrt{\frac{\text{counts}}{\text{second}}}$)	Variance	Mean/Variance
1	20.1000	4.8340	23.3676	0.8602
2	17.5056	4.1143	16.9275	1.0342
3	13.7000	3.6085	13.0213	1.0521
4	11.9333	3.5239	12.4179	0.9610
5	9.5111	3.1438	9.8835	0.9623
6	7.9333	2.8020	7.8512	1.0105
7	6.4778	2.7577	7.6049	0.8518
8	5.2333	2.3288	5.4233	0.9650
9	4.5000	2.0207	4.0832	1.1021
10	3.8833	2.1220	4.5029	0.8624

Table 8: Results from analysis of measurements of source blocked by varying thickness of lead